Imperfect Interfaces with Graded Materials and unilateral conditions: theoretical and numerical study

Serge Dumont[1] and Frédéric Lebon[2] and Raffaella Rizzoni[3]

Abstract
In this paper a composite body is considered. This body is made of three solids, two linear elastic adherents and a piecewise linear thin adhesive. The composite occupies a bounded domain depending naturally on a small parameter ε, which is the thickness, supposed constant, of the adhesive. Classically, it is possible to derive an interface imperfect law using asymptotic expansions as the thickness ε tends to zero. In this work, the material in the interphase is supposed to be graded, i.e. its elasticity properties vary along the thickness. Moreover, an unilateral condition is considered to avoid penetrations. A first result of the paper is that it is possible to apply the above methodology based on asymptotic expansions to this kind of materials. Then, a finite element method is introduced to solve the initial problem (with three layers) and the limit one (with two layers in imperfect contact). Various types of graded materials are numerically analyzed. In particular, different types of stiffness distributions are studied in detail.

Keywords
Interfaces, Micromechanics, Asymptotic expansions, Contact mechanics, Elasticity

[1]Université de Nîmes, IMAG - CNRS UMR 5149, Place E. Bataillon, 34095 Montpellier Cedex 5, France
[2]Aix-Marseille University, CNRS, Centrale Marseille, LMA, 4 Impasse Nikola Tesla, CS 40006, 13453 Marseille Cedex 13, France
[3]Dipartimento di Ingegneria, Università di Ferrara, Via Saragat 1, 44122 Ferrara, Italy

Corresponding author:
S. Dumont, Université de Nîmes, IMAG - CNRS UMR 5149, Place E. Bataillon, 34095 Montpellier Cedex 5, France
Email: serge.dumont@unimes.fr

Introduction

Functionally Graded Materials (FGM) are characterized by smooth variations of thermal, physical, chemical or/and mechanical properties [16], usually in a specific direction. These variations are due to gradual changes in composition, morphology and crystalline structure over volume. This kind of inhomogeneous revolutionary materials can be designed for particular, and often unique, function or applications. The overall properties of FGM are different from any of the constituents that form it. Nowadays, there is a wide range of real applications. Even if FGMs are typical in natural material (bone, teeth, etc.), the first technological development is due to Japanese researchers, who had to answer the challenge to create a material capable of bearing a thermal gradient of 1000 °C on a thickness of only 10 mm [14]. It is at present in the nuclear sector (thermonuclear fusion) that the need for the FGM is most vivid. Specifications (tenacity, heat resistance, strength to corrosion or irradiation) become more and more binding, often leading to contradictory requests that a unique monolithic material cannot perform. As an example, certain kind of steels are characterized by a conflict between the thermal resistance and the tenacity. In front of these requirements and as a supplement to the usual strategies of microstructure optimization, optimal designs based on material structuring at the mesoscopic scale are also explored. Other structural applications require a joint between two basic constituents, for example ceramic and metal (see fig. 1). This class of FGMs offers many advantages; in particular, the ceramic face is able of suppling high strength to wear, while the opposite metal face offers high hardness and mechanical strength. Such materials are expected to be very desirable for tribological applications, where wear resistance and high hardness are simultaneously required.
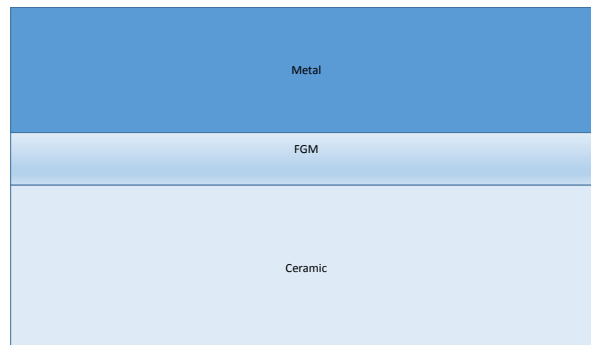

Figure 1. Example of Functionally Graded Material application: adhesive bonding of two basic constituents with specific thermic and mechanical properties.

In this paper, we are interested in modeling the behavior of FGM thin films, whose thickness is very small with respect to that of the adherents (metal and ceramic for example). The thickness of the FGM is consider as a small parameter and the limit problem is analyzed as the thickness tends to zero. In the present paper, a simple case is considered: the stiffness of the FGM linearly rescales with its thickness (soft material hypothesis). The limit problem is derived using matched asymptotic expansions [1,9–12,15]

and the obtained limit condition turns to be a law of imperfect interface. Here, the term *perfect interface* means that the jumps in the displacement and in the traction vectors across the interface are equal to zero. This situation arises for example when the rigidity of the interphase is of the same order of the rigidity of the adherents. On the contrary, the term *imperfect interface* means that either the jumps in the displacement or/and the jumps in the traction vectors are not vanishing. This last type of interface has been widely studied in previous works and in several applications (see for example [4–7])

The paper is divided in four parts. Section 2 is devoted to the mechanical problem and to some notations. In Section 3, an asymptotic analysis is performed in order to obtain a law of imperfect interface. The finite element implementation is presented in Section 4. Section 5 focuses on a numerical study of some academic examples.

The mechanical problem

Let us now consider the adhesive bonding of two linear elastic three dimensional bodies, where the mechanical properties of the adhesive may vary along the thickness (the third direction).

For that purpose, we define the following domains:

- $\Omega \subset I\!\!R^3$ is the whole structure, of boundary $\partial\Omega$;
- $B^\varepsilon = \{(x_1, x_2, x_3) \in \Omega : |x_3| < \frac{\varepsilon}{2}\}$ is the glue, also called the interphase;
- $\Omega_\pm^\varepsilon = \{(x_1, x_2, x_3) \in \Omega : \pm x_3 > \frac{\varepsilon}{2}\}$ are the adherents;
- $S_\pm^\varepsilon = \{(x_1, x_2, x_3) \in \Omega : x_3 = \pm\frac{\varepsilon}{2}\}$;
- $\Gamma = \{(x_1, x_2, x_3) \in \Omega : x_3 = 0\}$ is the interface, the geometrical limit of B^ε as ε vanishes;
- $B = \{(x_1, x_2, x_3) \in \Omega : |x_3| < \frac{1}{2}\}$ is the rescaled interphase;
- $\Omega_\pm = \{(x_1, x_2, x_3) \in \Omega : \pm x_3 > \frac{1}{2}\}$ are the adherents in the rescaled configuration;
- $S_\pm = \{(x_1, x_2, x_3) \in \Omega : x_\pm = \pm\frac{1}{2}\}$ are the surfaces between the adhesive and the adherents in the rescaled configuration;
- $\Omega_\pm^0 = \{(x_1, x_2, x_3) \in \Omega : \pm x_3 > 0\}$ are the domains occupied by the adherents in the limit configuration obtained as ε vanishes.

On a part Γ_1 of $\partial\Omega$, an external load g is applied, and on $\Gamma_0 \subset \partial\Omega$, such that $\Gamma_0 \cap \Gamma_1 = \emptyset$, a displacement u_d is imposed. Moreover, we suppose that $\Gamma_0 \cap B^\varepsilon = \emptyset$ and $\Gamma_1 \cap B^\varepsilon = \emptyset$. A body force f is applied in $\Omega_\pm^\varepsilon$. We consider also that the interface Γ is a plane normal to the third direction e_3. We are interested in the equilibrium of such a structure.

The equations of the mechanical problem are

$$\begin{cases} \text{div}\sigma^\varepsilon + f = 0 & \text{in } \Omega_\pm^\varepsilon \cup B^\varepsilon \\ \sigma^\varepsilon n = g & \text{on } \Gamma_1 \\ u^\varepsilon = u_d & \text{on } \Gamma_0 \\ \sigma^\varepsilon = A_\pm e(u^\varepsilon) & \text{in } \Omega_\pm^\varepsilon \\ \sigma^\varepsilon = A_i \left(e(u^\varepsilon)\right) & \text{in } B^\varepsilon \end{cases} \tag{1}$$

where $e(u^\varepsilon)$ is the strain tensor ($e_{ij}(u^\varepsilon) = \frac{1}{2}(u_{i,j} + u_{j,i})$, $i, j = 1, 2, 3$), $A_\pm$ are the elasticity tensors of the deformable adherents. Moreover, u^ε is considered as continuous across the interfaces S_+^ε and S_-^ε. The

piecewise linear operator A_i which defines the constitutive equation of the adhesive interphase is defined in the sequel. In the interphase B^ε, two isotropic regimes (traction vs compression) are considered:

$$\begin{cases} \sigma^\varepsilon & = \hat{\lambda} tr(e(u^\varepsilon))Id + 2\hat{\mu}e(u^\varepsilon) \ \ \text{if} \ \ tr(e(u^\varepsilon)) \geq 0 \\ \sigma^\varepsilon & = \bar{\lambda} tr(e(u^\varepsilon))Id + 2\hat{\mu}e(u^\varepsilon) \ \ \text{if} \ \ tr(e(u^\varepsilon)) \leq 0 \end{cases} \tag{2}$$

Let us emphasize that the strictly positive Lamé's coefficients of the interphase depend on the thickness ε of the interphase, i.e. we consider in this study that:

$$\hat{\lambda} = \lambda(x_3)\varepsilon, \ \hat{\mu} = \mu(x_3)\varepsilon, \ \bar{\lambda} = \bar{\lambda}(x_3) \tag{3}$$

As a consequence, in this study the adhesive has a non symmetric behaviour in traction (soft) and in compression (hard).

Asymptotic analysis

The thickness of the interphase being very small, we seek the solution of problem (1) using asymptotic expansions with respect to the small parameter ε:

$$\begin{cases} u^\varepsilon = u^0 + \varepsilon u^1 + O(\varepsilon^2) \\ \sigma^\varepsilon = \sigma^0 + \varepsilon \sigma^1 + O(\varepsilon^2) \end{cases} \tag{4}$$
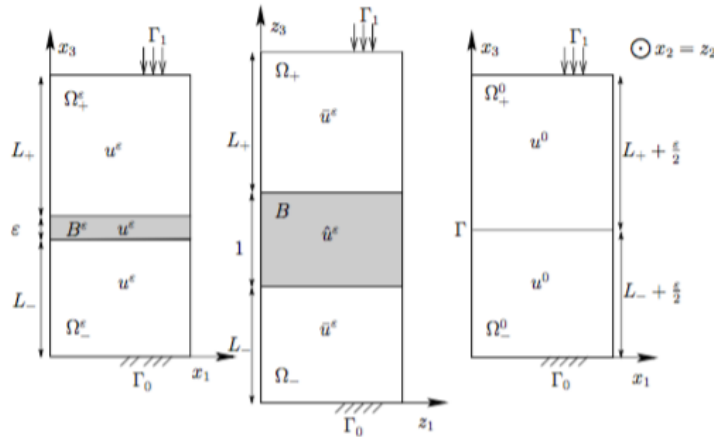

Figure 2. Geometry of the interphase/interface problem. Left: the initial problem with an interphase of thickness ε – Middle: the rescaled problem with interphase height equal to 1 in which the asymptotical analysis is realized – Right: the limit interface problem.

At this level, in order to work in a configuration independent of ε, the domain is rescaled using the classical procedure:

- In the glue, we define the following change of variable

$$(x_1, x_2, x_3) \in B^\varepsilon \to (z_1, z_2, z_3) \in B,$$
$$\text{with } (z_1, z_2, z_3) = (x_1, x_2, \frac{x_3}{\varepsilon})$$

(see configuration 2 of figure 2) and we denote $\hat{u}^\varepsilon(z_1, z_2, z_3) = u^\varepsilon(x_1, x_2, x_3)$ and $\hat{\sigma}^\varepsilon(z_1, z_2, z_3) = \sigma^\varepsilon(x_1, x_2, x_3)$.

- In the adherents, we define the following change of variable

$$(x_1, x_2, x_3) \in \Omega_+^\varepsilon \to (z_1, z_2, z_3) \in \Omega_+,$$
$$\text{with } (z_1, z_2, z_3) = (x_1, x_2, x_3 + 1/2 - \varepsilon/2)$$

and

$$(x_1, x_2, x_3) \in \Omega_-^\varepsilon \to (z_1, z_2, z_3) \in \Omega_-,$$
$$\text{with } (z_1, z_2, z_3) = (x_1, x_2, x_3 - 1/2 + \varepsilon/2)$$

We denote $\bar{u}^\varepsilon(z_1, z_2, z_3) = u^\varepsilon(x_1, x_2, x_3)$ and $\bar{\sigma}^\varepsilon(z_1, z_2, z_3) = \sigma^\varepsilon(x_1, x_2, x_3)$. We suppose that the external forces and the prescribed displacement u_d are assumed to be independent of ε. As a consequence, we define $\bar{f}(z_1, z_2, z_3) = f(x_1, x_2, x_3)$, $\bar{g}(z_1, z_2, z_3) = g(x_1, x_2, x_3)$ and $\bar{u}_d(z_1, z_2, z_3) = u_d(x_1, x_2, x_3)$.

- The classical matching at the interface adherent/adhesive is

$$u^0(x_1, x_2, 0^\pm) \approx u^0(x_1, x_2, \pm\varepsilon/2) = \hat{u}^0(x_1, x_2, \pm 1/2) = \bar{u}^0(x_1, x_2, \pm 1/2)$$
$$\sigma^0(x_1, x_2, 0^\pm) \approx \sigma^0(x_1, x_2, \pm\varepsilon/2) = \hat{\sigma}^0(x_1, x_2, \pm 1/2) = \bar{\sigma}^0(x_1, x_2, \pm 1/2) \tag{5}$$

From the equilibrium equation in the adhesive (eq. 1-1) it follows that

$$\hat{\sigma}_{ij,j}^\varepsilon = 0$$

and using (4), the $\frac{1}{\varepsilon}$ term in the development is identified as

$$\hat{\sigma}_{i3,3}^0 = 0,$$

leading to

$$[[\hat{\sigma}_{i3}^0]] = 0 \tag{6}$$

and

$$\hat{\sigma}_{i\alpha,\alpha}^0 = 0$$

for $i = 1, 2, 3$ and $\alpha = 1, 2$, where for a given function h, the following notation has been introduced: $[[h]] = h(z_1, z_2, +\frac{1}{2}) - h(z_1, z_2, -\frac{1}{2})$.

Let us consider the term $tr(e(u^\varepsilon))$, whose first term in the expansion (i.e. the $\frac{1}{\varepsilon}$ term) is $u_{3,3}^0$. Thus, after integration in the third direction, the two regimes, respectively $tr(e(u^\varepsilon)) \geq 0$ and $tr(e(u^\varepsilon)) \leq 0$,

lead to the conditions $\left[\left[u_3^0\right]\right] \geq 0$ and $\left[\left[u_3^0\right]\right] \leq 0$, respectively.

For the first regime (traction), the constitutive equation (2) at the first order of expansion (i.e. ε^0 term) gives

$$\begin{cases} (\lambda + 2\mu)\hat{u}_{3,3}^0 = \hat{\sigma}_{33}^0, \\ \mu\hat{u}_{\alpha,3}^0 = \hat{\sigma}_{\alpha 3}^0. \end{cases} \tag{7}$$

Because from (6), $\hat{\sigma}_{i3}^0$ is independent of x_3, we can rewrite these equalities as follows:

$$\begin{cases} \hat{u}_{3,3}^0 = \dfrac{1}{\lambda + 2\mu}\hat{\sigma}_{33}^0, \\[4mm] \hat{u}_{\alpha,3}^0 = \dfrac{1}{\mu}\hat{\sigma}_{\alpha 3}^0, \end{cases} \tag{8}$$

leading, by an integration over the interval $\left[-\frac{1}{2}, +\frac{1}{2}\right]$, to

$$\begin{cases} [[\hat{u}_3^0]] = \left(\displaystyle\int_{-\frac{1}{2}}^{\frac{1}{2}} \dfrac{1}{\lambda(x_3) + 2\mu(x_3)}dx_3\right)\hat{\sigma}_{33}^0, \\[5mm] [[\hat{u}_\alpha^0]] = \left(\displaystyle\int_{-\frac{1}{2}}^{\frac{1}{2}} \dfrac{1}{\mu(x_3)}dx_3\right)\hat{\sigma}_{\alpha 3}^0. \end{cases}$$

Then, by using the reverse change of variables (see for example [10] for more details) and the matching conditions (5), we can go back to $\Omega_\pm^0$ to obtain the following jump conditions across the interface at order zero

$$\begin{cases} \sigma_{33}^0 = \bar{M}\left[u_3^0\right] \ on \ \Gamma \\ \sigma_{\alpha 3}^0 = \bar{\mu}\left[u_\alpha^0\right] \ on \ \Gamma, \end{cases} \tag{9}$$

which hold on Γ when $\left[u_3^0\right] \geq 0$ and where we have defined the quantities

$$\begin{cases} \dfrac{1}{\overline{M}} = \dfrac{1}{\varepsilon}\displaystyle\int_{-\frac{\varepsilon}{2}}^{\frac{\varepsilon}{2}} \dfrac{1}{\lambda(x_3) + 2\mu(x_3)}dx_3 \\[5mm] \dfrac{1}{\bar{\mu}} = \dfrac{1}{\varepsilon}\displaystyle\int_{-\frac{\varepsilon}{2}}^{\frac{\varepsilon}{2}} \dfrac{1}{\mu(x_3)}dx_3 \end{cases} \tag{10}$$

with $[h] = \lim\limits_{x_3 \to 0^+} h(x_1, x_2, x_3) - \lim\limits_{x_3 \to 0^-} h(x_1, x_2, x_3)$ for a given function h.

For the second regime (compression), the constitutive equation gives

$$\hat{u}_{3,3}^0 = 0 \tag{11}$$

and thus,

$$\left[\left[\hat{u}_3^0\right]\right] = 0 \tag{12}$$

Then, going back to $\Omega^0_\pm$ and using the matching conditions (5), we obtain that

$$\left[u^0_3\right] = 0 \tag{13}$$

which holds when $\left[u^0_3\right] \leq 0$.

Using (2) and (11), it can be observed that the following conditions also hold for the second regime:

$$\begin{cases} \hat{u}^0_{1,1} + \hat{u}^0_{2,2} + \hat{u}^1_{3,3} \leq 0 \\ \hat{\sigma}^0_{33} = \bar{\lambda}\left(\hat{u}^0_{1,1} + \hat{u}^0_{2,2} + \hat{u}^1_{3,3}\right) + 2\mu\hat{u}^0_{3,3} = \bar{\lambda}\left(\hat{u}^0_{1,1} + \hat{u}^0_{2,2} + \hat{u}^1_{3,3}\right). \end{cases} \tag{14}$$

Thus we find $\hat{\sigma}^0_{33} \leq 0$ and using matching conditions (5), we further obtain that $\sigma^0_{33} \leq 0$ on Γ.
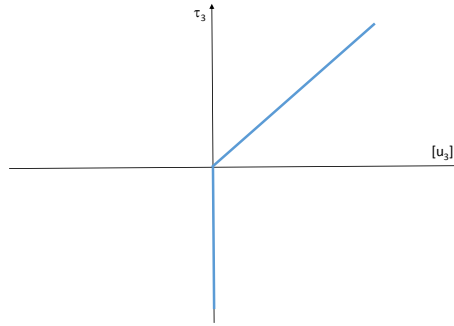

Figure 3. Unilateral contact law obtained by asymptotic expansions

To summarize, unilateral conditions of Signorini type are obtained (see fig. 3) and the approximated interface equilibrium problem at order 0 is as follows:

$$\begin{cases} \mathrm{div}\sigma^0 + f = 0 & \text{in } \Omega^0_\pm \\ \sigma^0 n = g & \text{on } \Gamma_1 \\ u^0 = u_d & \text{on } \Gamma_0 \\ \sigma^0 = A_\pm e(u^0) & \text{in } \Omega^0_\pm \\ \sigma^0 n = C\left[u^0\right]_+ + \tau^0 & \text{on } \Gamma \\ \left[u^0_3\right] \geq 0, \ \tau^0_3 \leq 0, \ \left[u^0_3\right]\tau^0_3 = 0 & \text{on } \Gamma \end{cases} \tag{15}$$

where

$$C = \begin{pmatrix} \bar{\mu} & 0 & 0 \\ 0 & \bar{\mu} & 0 \\ 0 & 0 & \bar{M} \end{pmatrix} \tag{16}$$

$$\tau^0 = \begin{pmatrix} 0 \\ 0 \\ \tau^0_3 \end{pmatrix} \tag{17}$$

and with

$$\left[u^0\right]_+ = \left(\begin{array}{c} \left[u_1^0\right] \\ \left[u_2^0\right] \\ \left[u_3^0\right] \end{array} \right) \tag{18}$$

if $\left[u_3^0\right] > 0$,

$$\left[u^0\right]_+ = \left(\begin{array}{c} \left[u_1^0\right] \\ \left[u_2^0\right] \\ 0 \end{array} \right) \tag{19}$$

if $\left[u_3^0\right] \leq 0$.

Finite element implementation and numerical tests

In this section, we propose a numerical procedure to solve problem (15). For the classical equations of elasticity in $\Omega_\pm^0$, a standard finite element method is used.

In order to properly take into account the jump conditions across the interface Γ, it is necessary to consider a test function v which can be discontinuous across the interface Γ. Multiplying the contact condition by the jump of this test function and integrating this relation among the interface, one obtains

$$\int_\Gamma [v]\sigma^0 n \, ds = \int_\Gamma [v]C[u^0] \, ds.$$

On the other hand, on each subdomain Ω_-^0 and Ω_+^0, we have

$$\int_{\Omega_\pm^0} e(v)A_\pm e(u^0) \, ds + \int_{\partial\Omega_\pm^0} v\sigma^0 n \, ds = 0.$$

Then adding the three last equalities (on Γ, Ω_-^0 and Ω_+^0), the weak formulation of problem (15) becomes

$$\int_{\Omega_\pm^0} e(v)A_\pm e(u^0) \, ds + \int_{\Gamma_1} vg \, ds + \int_\Gamma [v]C[u^0] \, ds = 0 \tag{20}$$

Finally, using a standard finite element method where the test functions are discontinuous across the interface, it is possible to write a stiffness matrix of problem (20) that is invertible and with standard error estimates (for more details, see for example[2,8,13]).

Numerical study

In this section, we propose a numerical study of the influence of the rigidity distribution in the glue on the overall structure behavior. For that purpose, we consider a two dimensional problem, derived from the three dimensional one using plane strain assumptions. In view of these considerations, the interface is now orthogonal to the second direction x_2 and the interface law (16) remains the same (see for example[2]). A solution of the mechanical problem described in the previous section for a particular stiffness distribution in the glue is represented in figure 5. The mesh is realized using the software GMSH[3].

In all the simulations below, the two adherents have the same material properties, with the Young's modulus equal to $E = 20000\ MPa$ and the Poisson's ratio equal to $\nu = 0.4$.

The adhesive consists of three phases with different glues, characterized by diverse rigidities and varying according to the numerical simulations.
The thickness of each phase is equal to $\varepsilon = 0.01m$.

The geometry of the mechanical problem is represented in figure 4, and an example of a solution is shown in figure 5.
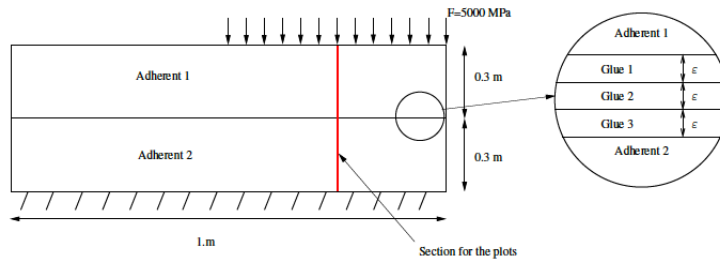
Figure 4. Geometry of the problem ($\varepsilon = 0$ for the interface problem)

In the simulations hereinafter, the subscript ε represents the solution of equilibrium problem (1) computed considering the interphase of thickness proportional to ε, whereas the subscript "soft,0" represent the solution of equilibrium problem (15) computed using the interface approximation at order 0 developed in the present paper.
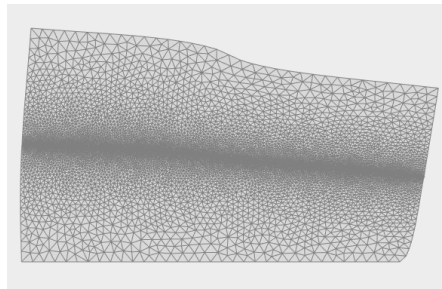

Figure 5. An example of a deformed structure, obtained considering the interphase problem made of three different phases

For the simulations considering the real three phases interphase, the finite element mesh contains 42,803 nodes and 21,314 finite elements (the total number of degree of freedom is equal to 85,468), whereas for the simulations with the interface law, the mesh consist of 11,186 elements and 22,530 nodes (the number of degrees of freedom is equal to 44,922).

Tests 1 (small rigidities for the glues)

In this first set of simulations, we consider a three phases interface, consisting of three glues with different rigidities that are all very small compared to those of the adherents.

Results for increasing rigidities In this paragraph, we consider a three phases interphase with a monotone distribution of rigidities, which are from 10 to 200 times smaller than those of the adherents (see table 1).

Table 1. Mechanical properties of the three phases of the interphase.

	Young's modulus	Poisson's ratio
Glue 1	2000 MPa	0.4
Glue 2	500 MPa	0.4
Glue 3	100 MPa	0.4

I will add the legend on the figures In the following figures, the displacement (figure 6) and the stress (figure 7) fields on the section drawn in figure 4 are represented. In figures 8 and 9, the jumps of the displacements and of the traction along the interface Γ are represented.
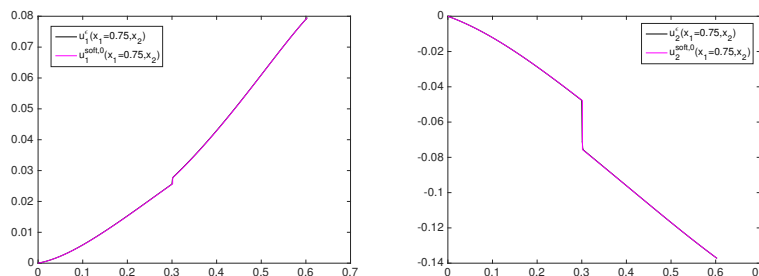

Figure 6. Displacements on the section (left: u_1, right: u_2): case of small and monotone distribution of rigidities for the glues.
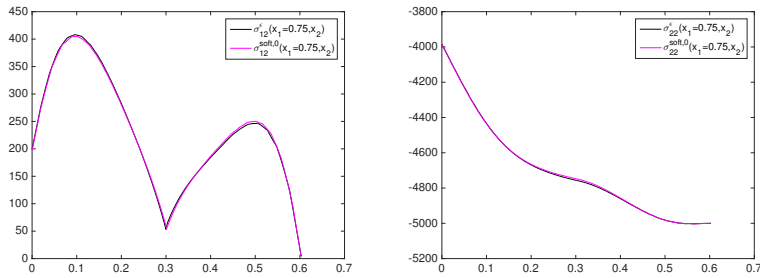
Figure 7. Stresses on the section (left: σ_{12}, right: σ_{22}): case of small and monotone distribution of rigidities for the glues.
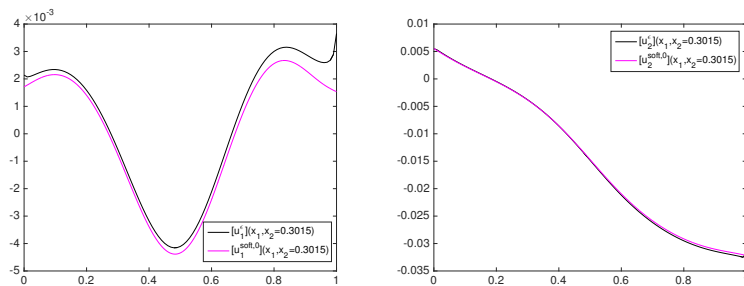

Figure 8. Jumps in the displacements across the interface (left: $[u_1]$, right: $[u_2]$): case of small and monotone distribution of rigidities for the glues.
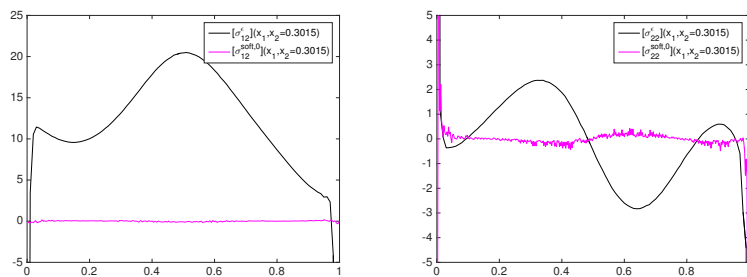

Figure 9. Jumps of the traction across the interface (left: $[\sigma_{12}]$, right: $[\sigma_{22}]$): case of small and monotone distribution of rigidities for the glues.

We can observe that, both in terms of displacements (cf. figure 6) and in terms of stress (cf. figure 7), the interface law is a very good approximation and correctly reproduces the overall behavior of

the structure. Moreover, figures 6 and 8 show that the jumps in the displacements across the interface $[u^\varepsilon]_\varepsilon := u^\varepsilon(x_1, \frac{\varepsilon}{2}) - u^2(x_1, -\frac{\varepsilon}{2})$ and $[u^{soft,0}]$ are numerically very close.

According to equation (6), the jumps in the stresses $[\sigma_{12}^{soft,0}]$ and $[\sigma_{22}^{soft,0}]$ have to be equal to zero across the interface. This is reproduced by our simulations, as it can be observed in figure 9. Consequently, the proposed finite element method is appropriated, and in the case of a very small rigidity of the glue in the interphase, the approximation that leads to consider a vanishing jumps in the constraint is justified. (To be developed ! $->$ give a ratio)

Results with non monotone rigidities In this paragraph, we consider a three phases interphase with rigidities much smaller than those of the adherents but now with a non monotone distribution, given in table 2.

Table 2. Mechanical properties of the three phases of the interphase.

	Young's modulus	Poisson's ratio
Glue 1	2000 MPa	0.4
Glue 2	100 MPa	0.4
Glue 3	500 MPa	0.4

In figures 10 to 13 we present some comparisons between the results obtained considering the three phases problem (1) and its approximated problem (15) using jumps in displacement across the interface Γ.
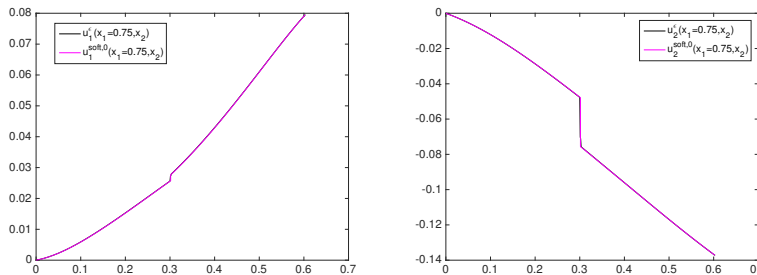

Figure 10. Displacements on the section (left: u_1, right: u_2): case of small and non monotone distribution of rigidities for the glues.
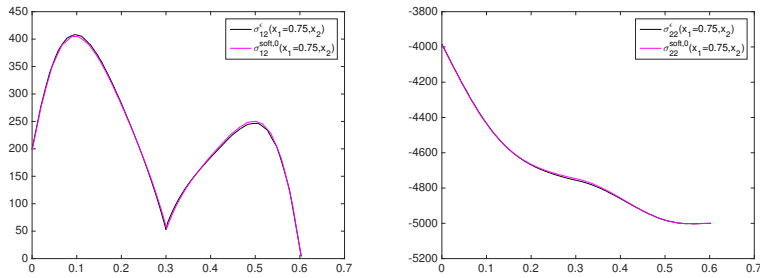
Figure 11. Stress on the section (left: σ_{12}, right: σ_{22}): case of small and non monotone distribution of rigidities for the glues.
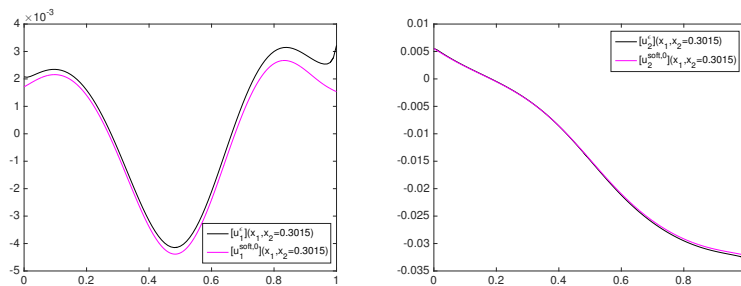

Figure 12. Jumps in the displacements across the interface (left: $[u_1]$, right: $[u_2]$): case of small and non monotone distribution of rigidities for the glues.
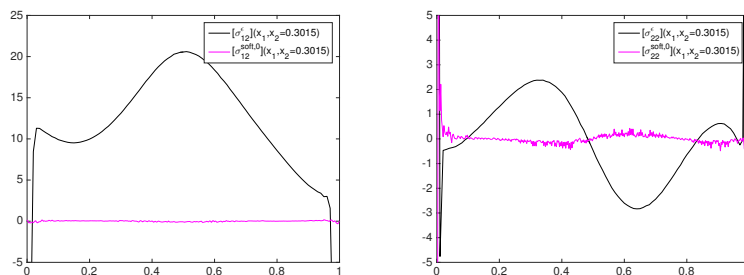

Figure 13. Jumps in the constraints across the interface (left: $[\sigma_{12}]$, right: $[\sigma_{22}]$): case of small and non monotone distribution of rigidities for the glues.

In figures 10 and 11, one can observe that the overall response of the structure is very similar than in the case of a monotone distribution of the rigidities in the interphase. The jumps, both in terms

of displacements (figure 12) and constraints (figure 13), are also very close for the two cases. As a consequence, the interface law given by formula (10) provides a good approximation of the behavior of the structure.

Comparison We compare here the results obtained with both monotone and non monotone distribution of the rigidities in the interphase. For that purpose, we present in figures 14 and 15 a zoom of the displacement and the constraint around the interphase, respectively.
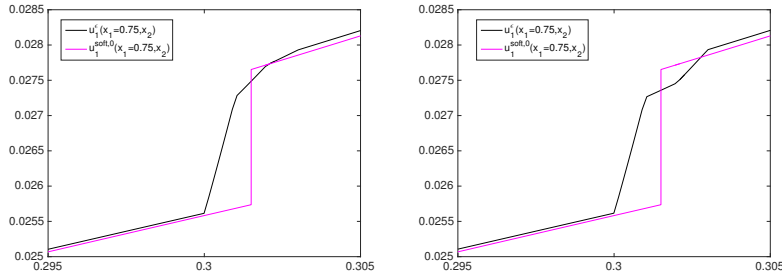

Figure 14. Displacements u_1 at the interface on the section for monotone (left) and non monotone (right) increasing rigidity
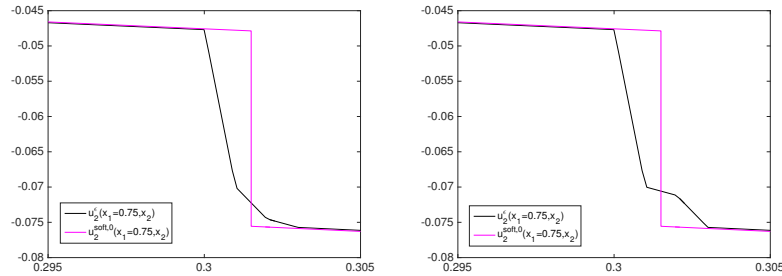

Figure 15. Displacements u_2 at the interface on the section for monotone (left) and non monotone (right) increasing rigidity

One can observe that we obtain very similar results for both monotone and non monotone rigidities in the glues, and the interface condition provides a very good approximation of the jumps both for the displacement and the constraint.

Tests 2 (very different rigidities for the glues)

We present in this section the results with an interphase in which the rigidity is strongly varying, from values close to the rigidity of the adherents to values much smaller.

In this case, we compare results with both a monotone (see table 3) and a non monotone (see table 4) rigidity distribution in the interphase.

Let us notice that, as in the previous example, the interface law is identical for the both cases, since it is given only by an average using formula (10).

Table 3. Mechanical properties of the three phases of the interphase: case of a monotone distribution of rigidities in the interphase

	Young's modulus	Poisson's ratio
Glue 1	10000 MPa	0.4
Glue 2	5000 MPa	0.4
Glue 3	1000 MPa	0.4

Table 4. Mechanical properties of the three phases of the interphase: case of a non monotone distribution of rigidities in the interphase

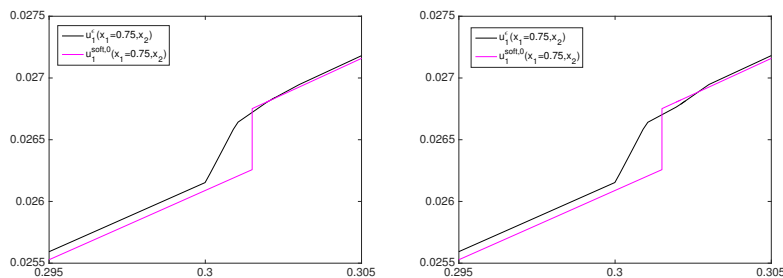|	Young's modulus	Poisson's ratio
Glue 1	10000 MPa	0.4
Glue 2	1000 MPa	0.4
Glue 3	5000 MPa	0.4

Figure 16. Zoom of the displacements u_1 at the interface on the section for monotone (left) and non monotone (right) increasing rigidity
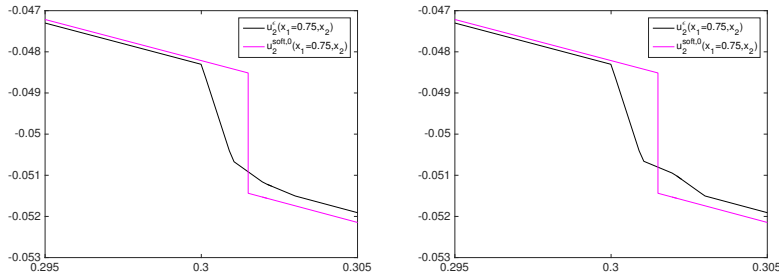
Figure 17. Zoom of the displacements u_2 at the interface on the section for monotone (left) and non monotone (right) increasing rigidity
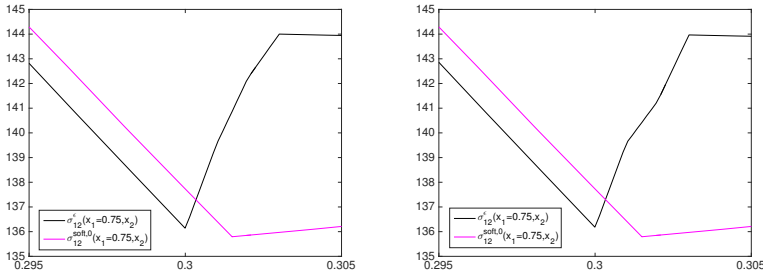

Figure 18. Zoom of the shear stress σ_{12} at the interface on the section for monotone (left) and non monotone (right) increasing rigidity

Figures 16,17,18 show zooms of the displacements u_1 and u_2 and the shear stress σ_{12} around the interphase. The jumps in the displacements $[u^\varepsilon]_e$ at the interphase are very similar for the two cases, even if we can observe the differences in the distribution of the rigidities inside the interphases (black curves in figures 16 and 17). Moreover, these jumps are correctly approximated by the interface law (red curves) and $[u^\varepsilon]_e$ and $[u^{soft,0}]$ are very close.

Concerning the shear stress, one can observe that the jumps at the interphase are similar for monotone and non monotone distribution. Moreover, the ratio between the jumps in the shear stress and the mean value of the shear stress around the interface is comparable to the previous ones, equal to $4 \cdot 10^{-2}$. Let us notice that in this test, the jumps in the stress σ_{22}, which is not represented here, is of the same order of the one obtained in the previous test.

Tests 3 (example with 5 different glues)

We now compare results obtained with two distributions of glues within the interface, provided respectively in table 5 and 6.

Table 5. Exemple with 5 glues in the interface: the monotone case

	Young's modulus	Poisson's ratio
Glue 1	1000 MPa	0.4
Glue 2	1000 MPa	0.4
Glue 3	1000 MPa	0.4
Glue 4	10000 MPa	0.4
Glue 5	10000 MPa	0.4

Table 6. Exemple with 5 glues in the interface: the non monotone case

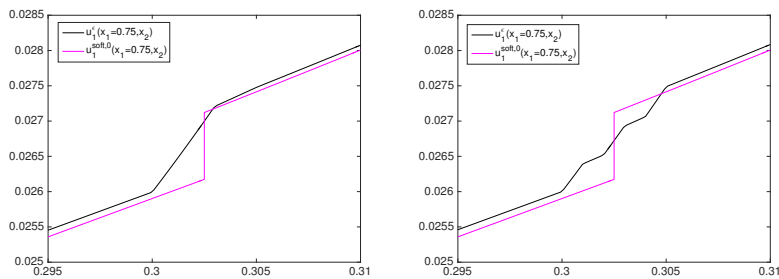|	Young's modulus	Poisson's ratio
Glue 1	1000 MPa	0.4
Glue 2	10000 MPa	0.4
Glue 3	1000 MPa	0.4
Glue 4	10000 MPa	0.4
Glue 5	1000 MPa	0.4

Figure 19. Zoom of the displacements u_1 around the interface on the section for monotone (left) and non monotone (right) increasing rigidity for interfaces made of 5 different glues

Figure 20. Zoom of the displacements u_2 around the interface on the section for monotone (left) and non monotone (right) increasing rigidity for interfaces made of 5 different glues
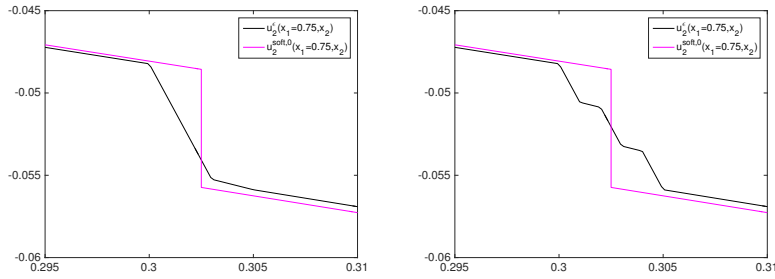

Figure 21. Zoom of the shear stress σ_{12} around the interface on the section for monotone (left) and non monotone (right) increasing rigidity for interfaces made of 5 different glues
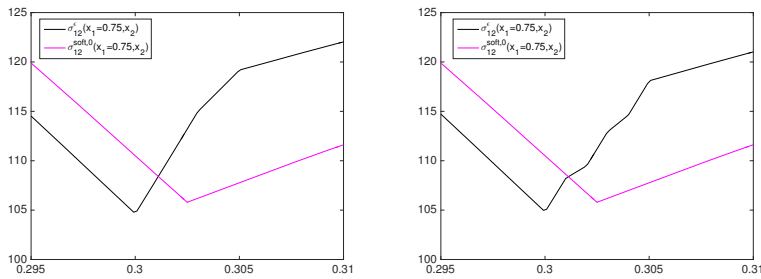
In figures 16, 19 and 21, one can observe that the results are very similar if the rigidity distribution is monotone or not, and the interface law provides a good approximation of what occurs in the interphase.

Tests 4: an exemple with traction

In this paragraph, we present an example of a structure with an adhesive composed by three layers, submitted to a a traction loading (see figure 22). The mechanical properties of each layer is provided in table 7. The distribution of the rigidity is not monotone.
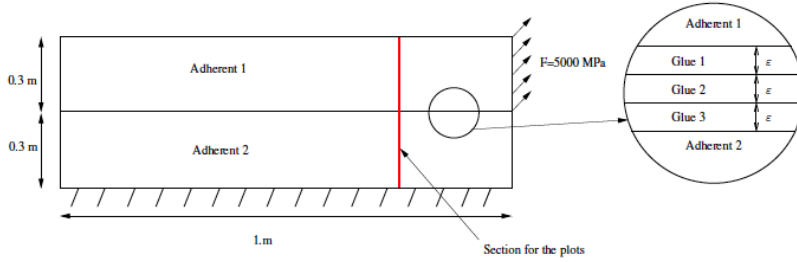
Figure 22. Geometry of the problem ($\varepsilon = 0$ for the interface problem)

Table 7. Mechanical properties of the three phases of the interphase: case of a monotone distribution of rigidities in the interphase

	Young's modulus	Poisson's ratio
Glue 1	1000 MPa	0.4
Glue 2	10000 MPa	0.4
Glue 3	5000 MPa	0.4

Figure 23 represents a zoom around the interface of the displacement u_1 (left) and the shear stress σ_{12} (right). One can observe that, in this situation, the approximation of the multi-layers initial problem is correctly approximated by the soft interface modeling proposed in the first part of the paper.
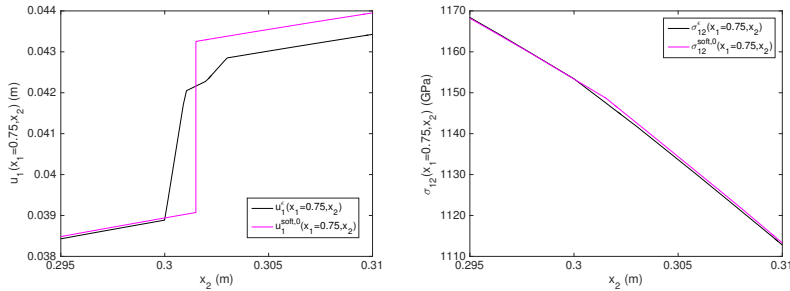

Figure 23. Zoom of the displacement u_1 (left) the shear stress σ_{12} (right) around the interface on the section for non monotone rigidity for interfaces made of 3 different glues submitted to a traction loading

Conclusion on the numerical results

In all the numerical examples presented, one can observe that the interface law given in (10) and in (15) always provides a good approximation of the initial multi-phase problem, even if some of the layers on

the interphase are rigid (which is not the case in the theory where the stiffness is of order ε), or if the rigidity distribution in the interphase is not monotone.

Conclusion

In this paper, we have presented a study of a composite made of three elastic bodies, two adherents and a thin adhesive. The elastic properties of the adhesive are supposed to depend on the thickness direction and to have two regimes, one in traction (soft) and one in compression (hard). After the derivation of an interface law for such a structure, we have numerically compared the response of the initial three phases composite and the approximated one, using two phases and an interface law. We have shown that the responses for low thickness (with a ratio 0.01 mm/0.3 m) are in a good agreement, especially in terms of displacements, for various distributions of rigidities in the adhesive, and even if the rigidity in some parts of the adhesive is of the same order of that of the adherents.

References

1. R. Abdelmoula, M. Coutris, and J.J. Marigo. Comportement asymptotique d'une interface mince. *Compte Rendu Académie des Sciences Série IIB*, 326:237–242, 1998.
2. S. Dumont, F. Lebon, and R. Rizzoni. An asymptotic approach to the adhesion of thin stiff films. *Mechanics Research Communications*, 58:24–35, 2014.
3. C. Geuzaine and J.-F. Remacle. Gmsh: a three-dimensional finite element mesh generator with built-in pre- and post-processing facilities. *Int. J. Numer. Meth. Engng.*, 679:1309–1331, 2009.
4. Z. Hashin. Thin interphase/imperfect interface in conduction. *Journal of Applied Physics*, 89, 2001.
5. Z. Hashin. Thin interphase/imperfect interface in elasticity with application to coated fiber composites. *Journal of the Mechanics and Physics of Solids*, 50, 2002.
6. A. Javili, S. Kaessmair, and P. Steinmann. General imperfect interfaces. *Computer Methods in Applied Mechanics and Engineering*, 275, 2014.
7. A. Javili, P. Steinmann, and J. Mosler. Micro-to-macro transition accounting for general imperfect interfaces. *Computer Methods in Applied Mechanics and Engineering*, 317, 2017.
8. F. Lebon, A. Ould Khaoua, and C. Licht. Numerical study of soft adhesively bonded joints in finite elasticity. *Comput. Mech.*, 21:134–140, 1997.
9. F. Lebon and R. Rizzoni. Asymptotic study of a soft thin layer: the non convex case. *Mech. Adv. Mat. Struct.*, 15:12–20, 2008.
10. F. Lebon and R. Rizzoni. Asymptotic behavior of a hard thin linear interphase: An energy approach. *Int. J. Solids Struct.*, 48:441–449, 2011.
11. F. Lebon and R. Rizzoni. Modelling adhesion by asymptotic techniques. *Adhesive Properties in Nanomaterials, Composites and Films*, pages 96–126, 2011.
12. C. Licht and G. Michaille. A modeling of elastic adhesive bonded joints. *Adv. Math. Sci. Appl.*, 7:711–740, 1997.
13. J.A. Nairn. Numerical implementation of imperfect interfaces. *Computational Materials Science*, 40:525–536, 2007.
14. M. Niino, T. Hirai, and R. Watanabe. The functionally gradient materials. *J. Jap. Soc. Compos. Mat.*, 13:257–264, 1984.

15. E. Sanchez-Palencia. *Non-homogeneous media and vibration theory*. Lecture Notes in Physics 127, Spriger-Verlag, 1980.

16. G. Udupa, S. Shrikantha Rao, and K.V. Gangadharan. Functionally graded composite materials: An overview. *Procedia Materials Science*, 5:1291–1299, 2014.